JACS
JOURNAL OF THE AMERICAN CHEMICAL SOCIETY
Article
Cite This: J. Am. Chem. Soc. 2018, 140, 2656−2664
pubs.acs.org/JACS

Benzoyl Halides as Alternative Precursors for the Colloidal Synthesis of Lead-Based Halide Perovskite Nanocrystals

Muhammad Imran,[†,‡] Vincenzo Caligiuri,[†] Mengjiao Wang,[†,‡] Luca Goldoni,[§,∥] Mirko Prato,[⊥] Roman Krahne,[†] Luca De Trizio,*[,†] and Liberato Manna*[,†]

[†]Nanochemistry Department, [§]D3 PharmaChemistry Line Department, [∥]Analytical Chemistry Facility and [⊥]Materials Characterization Facility, Istituto Italiano di Tecnologia (IIT), Via Morego 30, 16163 Genova, Italy

[‡]Dipartimento di Chimica e Chimica Industriale, Università degli Studi di Genova, Via Dodecaneso 31, 16146 Genova, Italy

Supporting Information

ABSTRACT: We propose here a new colloidal approach for the synthesis of both all-inorganic and hybrid organic−inorganic lead halide perovskite nanocrystals (NCs). The main limitation of the protocols that are currently in use, such as the hot injection and the ligand-assisted reprecipitation routes, is that they employ PbX_2 (X = Cl, Br, or I) salts as both lead and halide precursors. This imposes restrictions on being able to precisely tune the amount of reaction species and, consequently, on being able to regulate the composition of the final NCs. In order to overcome this issue, we show here that benzoyl halides can be efficiently used as halide sources to be injected in a solution of metal cations (mainly in the form of metal carboxylates) for the synthesis of $APbX_3$ NCs (in which A = Cs^+, $CH_3NH_3^+$, or $CH(NH_2)_2^+$). In this way, it is possible to independently tune the amount of both cations and halide precursors in the synthesis. The $APbX_3$ NCs that were prepared with our protocol show excellent optical properties, such as high photoluminescence quantum yields, low amplified spontaneous emission thresholds, and enhanced stability in air. It is noteworthy that $CsPbI_3$ NCs, which crystallize in the cubic α phase, are stable in air for weeks without any postsynthesis treatment. The improved properties of our $CsPbX_3$ perovskite NCs can be ascribed to the formation of lead halide terminated surfaces, in which Cs cations are replaced by alkylammonium ions.

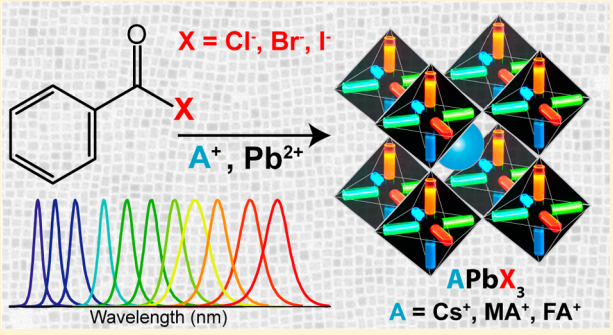

INTRODUCTION

Over the past few years, semiconductor metal halide nanocrystals (NCs) with a perovskite crystal structure have emerged as one of the most interesting materials for optoelectronic applications.[1−11] In particular, lead-based halide perovskite NCs with formula $APbX_3$, in which A can be Cs^+, $CH_3NH_3^+$ (MA), or $CH(NH_2)_2^+$ (FA) and X is Cl, Br, or I, have been recently shown to have outstanding optical properties.[12] Such compounds are characterized by a broad tunable photoluminescence (PL) that ranges from the ultraviolet (UV) to the near-infrared region of the electromagnetic spectrum, a narrow full width at half-maximum (fwhm), and high PL quantum yields (PLQY).[7−11,13−19] Interestingly, the PL emission of such perovskite NCs can be easily adjusted not only through size control and subsequently through quantum confinement, as is the case for standard quantum dots but also through compositional mixing, for example, via simple anion-exchange reactions.[20−27] Such properties have inspired researchers to exploit this class of materials for use in efficient solar cells, sensitive photodetectors, low threshold lasers, and light-emitting diodes (LEDs).[3,4,7,9−13]

To date, various approaches have been proposed for the direct synthesis of all-inorganic and organic−inorganic metal halide perovskite colloidal NCs, with the hot-injection and the ligand-assisted reprecipitation (LARP) ones being the most used and most developed methods.[7,9−11] The former, which was initially devised for all-inorganic perovskite NCs, is based on the hot injection (up to 200 °C) of the A cation (in the form of Cs−oleate for Cs or methylamine for MA) to a solution containing a metal halide salt (e.g., PbX_2, X = Cl, Br, I) and surfactants (e.g., oleylamine and oleic acid).[19,28−33] Immediately after the injection, a rapid salt metathesis reaction occurs, forming ternary halide NC materials. Conversely, the LARP strategy, which was originally proposed for the synthesis of organic−inorganic $MAPbX_3$ NCs, but was later extended to the synthesis of all-inorganic $CsPbX_3$ systems, is performed at low temperatures (typically from room temperature, RT, to 60 °C). This method is based on the reprecipitation of halide salts in the presence of ligands: metal halide salts (or organic halide salts in the case of hybrid perovskites) are solubilized in one or more polar solvents, like DMF, and are subsequently added dropwise to a nonpolar medium, like toluene, in the presence of ligands.[2,15,18,34−40] The low solubility of halide salts in the nonpolar solvent triggers their precipitation with the recrystallization of halide NCs.

Received: December 20, 2017
Published: January 29, 2018

DOI: 10.1021/jacs.7b13477
J. Am. Chem. Soc. 2018, 140, 2656−2664

Both procedures have various limitations, the main one of which is the use of inorganic salts (i.e., PbX_2) as both cation and anion precursors. Indeed, since the ratio of cations to anions employed in the synthesis is linked to that of the chosen inorganic salts, it is not possible to precisely tune the composition of the final NCs. Furthermore, a notable disadvantage is that it is difficult to work with an excess of halide ions, which is an experimental condition that has been shown to favor the formation of lead halide perovskite NCs with improved stability and optical properties.[2,29,41]

The obstacles imposed by these two techniques were partially overcome by Wei et al., who proposed an alternative colloidal route for the preparation of $CsPbX_3$ NCs, which was later called the "three-precursors approach".[42] Such a synthesis is based on the dissolution of Cs^+ and Pb^{2+} cations in fatty acids followed by the injection of an alkylammonium halide salt (as the halide precursor). This procedure was then adopted and revised by Yassitepe et al. for the preparation of amine-free $CsPbX_3$ NCs for LEDs[43] and by Protesescu et al. and Li et al. for the synthesis of $FAPbX_3$ (X = Br, I) NCs.[44−46] This approach allows one to work with the desired stoichiometry of the ions, since the halide ions and the metal cation sources are not delivered together, i.e., they are not delivered with the same chemical precursor. On the other hand, its potential versatility is limited by the poor reactivity of the alkylammonium halide salts (i.e., $CsPbI_3$, $CsPbCl_3$, $MAPbX_3$, and $FAPbCl_3$ NCs have not been reported using this strategy), which can also lead to the formation of undesired secondary phases.

In order to overcome the restrictions associated with the aforementioned synthetic procedures, we propose here a new colloidal synthesis approach that can lead to either all-inorganic or organic−inorganic lead-based halide perovskite NCs. This new approach relies on the use of benzoyl halides as halide precursors, which can be easily injected into a solution of metal cations (such as metal carboxylates) and desired ligands (oleylamine and oleic acid). This injection immediately triggers the nucleation and the growth of metal halide NCs (see Scheme 1). By simply tuning the relative amount of cation precursors, ligands, solvents, benzoyl halides, and the injection temperature, it is possible to synthesize either all-inorganic or organic−inorganic $APbX_3$ (A = Cs, MA or FA and X = Cl, Br or I) NCs with tight control over the size distribution and with high phase purity. In addition, thanks to the strong reactivity of benzoyl halides even at RT, they can be used for anion-exchange reactions using presynthesized $CsPbX_3$ NCs.

Scheme 1. Colloidal Synthesis of Lead Based Halide Perovskite Nanocrystals Using Benzoyl Halides as Halide Precursors

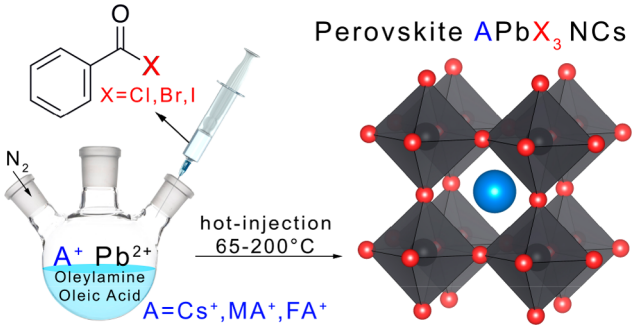

The $APbBr_3$ NCs that were prepared using our protocol are characterized by their PLQYs, which were as high as 92%, and by their very low amplified spontaneous emission (ASE) thresholds. Moreover, the $APbI_3$ NCs had PLQYs of around 55% and, finally, the $CsPbCl_3$ NCs exhibited a record PLQY value of 65%. Also, they exhibited a much higher phase stability than that which has been previously reported for NCs prepared with other synthesis methods. It is noteworthy that cubic $CsPbI_3$ NCs are stable in air for weeks without any postsynthetic treatment, which is different from those prepared using the classic hot-injection or LARP approaches.[28,44,47−50] The optimal properties of our $CsPbX_3$ perovskite NCs can be ascribed to the formation of lead halide-terminated surfaces in which Cs cations are replaced by alkylammonium ions. Our X-ray photoelectron spectroscopy analysis revealed, in fact, that all our $CsPbX_3$ NCs are Cs poor and contain a considerable amount of amines, most likely in the form of oleylammonium ions. Indeed, the formation of these surfaces is favored under our synthetic conditions: the use of benzoyl halides provides a halide-rich environment and, at the same time, an efficient protonation of the oleylamine.

EXPERIMENTAL SECTION

Chemicals. Lead acetate trihydrate ($Pb(CH_3COO)_2{\cdot}3H_2O$, 99.99%), lead(II) oxide (PbO, 99.999%), sodium iodide (NaI, 99.99%) cesium carbonate (Cs_2CO_3, reagent Plus, 99%), cesium acetate (CH_3COOCs, 99.9%), methylamine (CH_3NH_2, 2 M solution in tetrahydrofuran, THF), formamidinium acetate salt ($HN{=}CHNH_2{\cdot}CH_3COOH$, 99%), benzoyl bromide (C_6H_5COBr, 97%), benzoyl chloride (C_6H_5COCl, 98%), toluene (anhydrous, 99.5%), octadecene (ODE, technical grade, 90%), oleylamine (OLAM, 70%), and oleic acid (OA, 90%) were purchased from Sigma-Aldrich. All chemicals were used without any further purification.

Preparation of Benzoyl Iodide. The reaction was performed in a N_2-filled glovebox following the procedure reported by Theobald and Smith.[51] In short, sodium iodide (3 g) was mixed with benzoyl chloride (1.4 mL) in a 20 mL vial. The mixture was vigorously stirred at 75 °C on a hot plate for 5 h. The reaction mixture turned from colorless to an orange red color, indicating that the transformation of the benzoyl chloride into the benzoyl iodide was successful. Next, the reaction mixture was cooled down to RT and diluted using 3 mL of anhydrous ODE. Finally, the solution was filtered, using a polytetrafluorethylene membrane filter with a 0.45 μm pore size, in order to collect the liquid precursor. The unambiguous identification of all of the organic species in solution as well as the reaction yield (97.7%) was possible by means of nuclear magnetic resonance (NMR, see the Supporting Information, SI, for the complete assignment and quantification of the species in the reaction mixture).

Synthesis of $CsPbX_3$ NCs. In a typical synthesis, cesium carbonate (16 mg), lead acetate trihydrate (76 mg), 0.3 mL of OA, 1 mL of OLAM, and 5 mL of ODE were loaded into a 25 mL 3-neck round-bottom flask and dried under vacuum for 1 h at 130 °C. Subsequently, the temperature was increased to 165−200 °C (See Table 1 for details) under N_2, and the desired amount of the benzoyl halide precursor was swiftly injected (0.6 mmol in the case of benzoyl bromide and iodide and 1.8 mmol in the case of benzoyl chloride). The reaction mixture was immediately cooled down in an ice−water bath for $CsPbBr_3$ and $CsPbI_3$ NCs, while it was quenched after 20 s for $CsPbCl_3$ NCs. Finally, 5 mL of toluene was added to the crude NC solutions, and the resulting mixture was centrifuged for 10 min at 4 krpm. The supernatant was discarded, and the precipitate was redispersed in 5 mL of toluene for further use.

Synthesis of Mixed $CsPb(Br,Cl)_3$ and $CsPb(Br,I)_3$ NCs. Cesium carbonate (16 mg), lead acetate trihydrate (76 mg), 0.3 mL of OA, 1 mL of OLAM, and 5 mL of ODE were loaded into a 25 mL 3-neck round-bottom flask and dried under vacuum for 1 h at 130 °C. Subsequently, the temperature was increased to 170 °C under N_2, and

DOI: 10.1021/jacs.7b13477
J. Am. Chem. Soc. 2018, 140, 2656−2664

Table 1. Synthetic Parameters Used for the Synthesis of $APbX_3$ NCs

sample	OLAM (mL)	OA (mL)	temperature (°C)
$CsPbCl_3$	1	0.3	200
$CsPbBr_3$	1	0.3	170
$CsPbI_3$	1	0.3	165
$MAPbCl_3$	0.1	2.5	65
$MAPbBr_3$	0.025	2.5	65
$MAPbI_3$	0.150	2.5	65
$FAPbCl_3$	0.025	2.5	95
$FAPbBr_3$	0.025	2.5	75
$FAPbI_3$	0.200	2.5	95

0.6 mmol of the mixture of benzoyl chloride/bromide (a precursor ratio of 1:1 led to NCs emitting at 448 nm) or benzoyl bromide/iodide (precursor ratios of 5:1 and 1:1 led to NCs emitting at 544 and 594 nm, respectively) was swiftly injected. The reaction mixture was immediately cooled down in an ice−water bath. The NCs were collected by adding 5 mL of toluene to the crude solution followed by centrifugation at 4 krpm for 10 min. The supernatant was discarded, and the precipitate was redispersed in 5 mL of toluene.

Synthesis of $MAPbX_3$ NCs. Lead oxide (44 mg), 2.5 mL of OA, 0.025 mL of OLAM, and 5 mL of ODE were mixed in a 25 mL 3-neck round-bottom flask and dried under vacuum for 1 h at 125 °C. Subsequently, the temperature was lowered to 65 °C under N_2. Methylamine (0.170 mL) was injected, followed by the injection of 0.6 mmol of the benzoyl halide precursor (see Table 1 for details). The reaction was quenched by the addition of 5 mL of toluene after 30 s in the case of $MAPbBr_3$ and $MAPbI_3$ NCs and after 10 s in the case of $MAPbCl_3$ NCs. The NCs were collected by centrifuging the crude solution at 4 krpm for 10 min.

Synthesis of $FAPbX_3$ NCs. Lead acetate trihydrate (76 mg), formamidinium acetate (40 mg), 2.5 mL of OA, 0.025 mL of OLAM, and 5 mL of ODE were mixed in a 25 mL 3-neck round-bottom flask and dried under vacuum for 1 h at 125 °C. Subsequently, the temperature was lowered to 75−95 °C (See table S1) under N_2, and 0.6 mmol of the benzoyl halide precursor was rapidly injected. After 30 s, the reaction mixture was cooled down in an ice−water bath. A 5 mL amount of toluene was added to the crude solution, and the resulting mixture was centrifuged for 10 min at 4 krpm. $FAPbI_3$ NCs were washed once with ethyl acetate (using a toluene/ethyl acetate ratio of 5/1) and were eventually redispersed in toluene.

Anion Exchange Reactions. In short, 0.500 mL of the $CsPbX_3$ NC dispersion was diluted with 2 mL of anhydrous toluene, and different amounts of a 0.12 M solution of benzoyl halide in toluene (ranging from 30 to 500 μL) were swiftly injected under vigorous stirring at RT. Finally, the NCs were collected by centrifugation at 4 krpm for 10 min.

UV−vis Absorption and PL Measurements. The UV−vis absorption spectra were recorded using a Varian Cary 300 UV−vis absorption spectrophotometer. The PL spectra were measured on a Varian Cary Eclipse spectrophotometer using an excitation wavelength (λ_{ex}) of 350 nm for all of the chloride and bromide samples and 450 nm for all of the iodide compounds. Samples were prepared by diluting NC solutions in toluene in quartz cuvettes with a path length of 1 cm.

PL Quantum Yields and Time-Resolved PL Measurements. The samples were measured with an Edinburgh FLS900 fluorescence spectrometer equipped with a xenon lamp, a monochromator for steady-state PL excitation, and a time-correlated single-photon counting unit coupled with a pulsed laser diode (λ_{ex} = 375 and 405 nm, pulse width = 50 ps) for time-resolved PL. The PLQY was measured using a calibrated integrating sphere (λ_{ex} = 350 nm for all of the chloride and the bromide samples and λ_{ex} = 450 nm for all of the iodide samples). All solutions were diluted to an optical density of 0.1 or lower (at the corresponding excitation wavelength) in order to minimize the reabsorbance of the fluorophore.

Amplified Spontaneous Emission (ASE) Measurements. All of the $APbBr_3$ (A = Cs^+, MA^+, or FA^+) NC samples that were used for ASE dynamics were cleaned twice by precipitation using ethyl acetate (the volume ratio of toluene to ethyl acetate was 5:1) and redispersion in toluene. Eventually, thick NC films were produced on glass substrates by drop casting the colloidal solutions. The NC films were optically excited by a pulsed laser source at λ = 405 nm, with a pulse width of 50 fs and a repetition rate of 1 kHz at normal incidence. The pump beam was focused on the sample by a cylindrical lens, producing an excitation stripe of about 0.6 cm in length. The emission spectra were recorded using a collection lens and a fiber-coupled Ocean Optics HR4000 spectrometer at an angle close to 90° with respect to that of the excitation beam.

Transmission Electron Microscopy (TEM) Characterization. The samples were prepared by drop-casting dilute solutions of NCs onto carbon-coated copper grids. Low-resolution TEM measurements were performed on a JEOL-1100 transmission electron microscope operating at an acceleration voltage of 100 kV.

X-ray Diffraction (XRD) Characterization. XRD analysis was performed on a PANanalytical Empyrean X-ray diffractometer, equipped with a 1.8 kW Cu Kα ceramic X-ray tube and a PIXcel^{3D} 2 × 2 area detector, operating at 45 kV and 40 mA. Specimens for the XRD measurements were prepared by drop-casting a concentrated NC solution onto a quartz zero-diffraction single crystal substrate. The diffraction patterns were collected under ambient conditions using parallel beam geometry and symmetric reflection mode. XRD data analysis was conducted using the HighScore 4.1 software from PANalytical.

X-ray Photoelectron Spectroscopy (XPS) Characterization. Measurements were performed on a Kratos Axix Ultra DLD spectrometer using a monochromatic Al Kα source (15 kV, 20 mA). The photoelectrons were detected at a takeoff angle of ϕ = 0° with respect to the surface normal. The pressure in the analysis chamber was maintained below 7×10^{-9} Torr for data acquisition. The data was converted to VAMAS format and processed using CasaXPS software, version 2.3.17. The binding energy (BE) scale was internally referenced to the C 1s peak (BE for C−C = 284.8 eV).

RESULTS AND DISCUSSION

The synthetic strategy we propose here was inspired by the one employed for the nonaqueous synthesis of metal oxide NCs.[52] In a typical synthesis of metal oxide NCs, the release of water, i.e., the oxygen precursor, can be achieved by reacting carboxylic acids with either amines or alcohols at relatively high temperatures (above 200 °C), as illustrated by eqs 1 and 2.

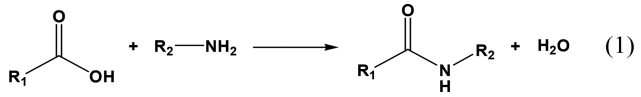

(1)

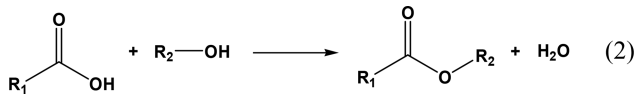

(2)

Similarly, acyl halides are well known for their strong reactivity toward nucleophilic compounds (i.e., amines, alcohols, carboxylic acids) which form carboxylic acid derivatives even at room temperature (i.e., amides, esters, anhydrides) and simultaneously release hydrohalic acids (see eqs 3−5).[53]

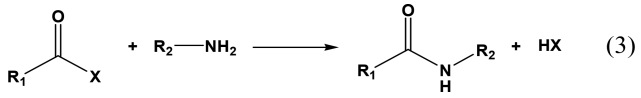

(3)

DOI: 10.1021/jacs.7b13477
J. Am. Chem. Soc. 2018, 140, 2656−2664

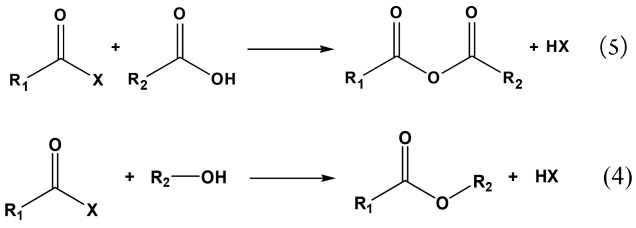

Thus, the idea behind our colloidal approach is to inject acyl halide molecules into a solution of metal cations that have been dissolved in nucleophilic molecules, namely, amines and carboxylic acids, at a desired temperature, in order to trigger the release of halide ions and, consequently, the nucleation and growth of metal halide NCs. Among the possible acyl halide molecules, we selected benzoyl halides since they are low cost and have a sufficiently high boiling point (~200 °C), which allows for the synthesis of metal halide NCs even at relatively high temperatures. Furthermore, considering the strong reactivity of acyl halides toward nucleophilic species, another important aspect of benzoyl halides is that they are more stable than aliphatic acyl halides as a result of their stabilization by the π-overlap in the ground state.[54] Indeed, the more stable the anion precursor is, the more controlled the release of the halide ions should be, which, in turn, could lead to the fine tuning of the size distribution of the NC.[55]

In order to understand the efficacy of our synthetic protocol, we tested the synthesis of lead-based halide perovskites NCs, paying particular attention to the optimization of their phase purity, size distribution, and optical properties. To this end, we chose to synthesize the benzoyl iodide precursor due to the commercial availability of only the benzoyl chloride and bromide compounds. This precursor can be easily prepared by reacting benzoyl chloride with anhydrous sodium iodide at 75 °C in an inert atmosphere (see Experimental Section and Figure S1 of the SI).[51,56]

First, we will illustrate the results obtained for $CsPbX_3$ NCs. In a typical synthesis, cesium carbonate and lead acetate were dissolved and degassed in oleylamine, oleic acid, and octadecene at 130 °C in a three-neck flask. Subsequently, the solution was heated up to the desired temperature (170–200 °C), and the benzoyl halide precursor was swiftly injected into the reaction flask, triggering the immediate nucleation and growth of the NCs (see Experimental Section and Table 1). Bright-field TEM images of $CsPbX_3$ NCs show that the crystals had a cubic shape and a narrow size distribution (see Figure 1a–c and Figure S2 of the SI). The average size of the $CsPbCl_3$ NCs was 8.6 ± 1.0 nm, while it was 7.8 ± 1.3 nm for the $CsPbBr_3$ ones and 10.1 ± 1.6 nm for the $CsPbI_3$ ones.

The XRD patterns of $CsPbX_3$ NCs nicely match the cubic perovskite structure ($CsPbBr_3$ ICSD code 29073, $CsPbCl_3$ ICSD code 23108, $CsPbI_3$ ICSD code 181288) in all three cases, and no secondary phases were present (see Figure 1d–f). Remarkably, the $CsPbX_3$ NCs exhibited a narrow PL emission line width, ranging from 11 ($CsPbCl_3$), to 18 ($CsPbBr_3$), to 32 nm ($CsPbI_3$) and had PLQYs as high as 92% (see Figure 1g–i). $CsPbCl_3$ NCs were of particular interest: while cesium lead chloride perovskite NCs are typically characterized by a significant nonradiative decay, the PLQY of $CsPbCl_3$ NCs was measured to be as high as 65%, which is a record value.[16,57] It is important to highlight that such a high PLQY was observed only when employing a large excess of the Cl precursor, i.e., 1.8 mmol of benzoyl chloride and 0.2 mmol of the Pb precursor (see the Experimental Section). On the other hand, $CsPbCl_3$ NCs were characterized by a weak PL emission when they were prepared using a lower amount of benzoyl chloride. For example, using 0.6 mmol of benzoyl chloride and 0.2 mmol of

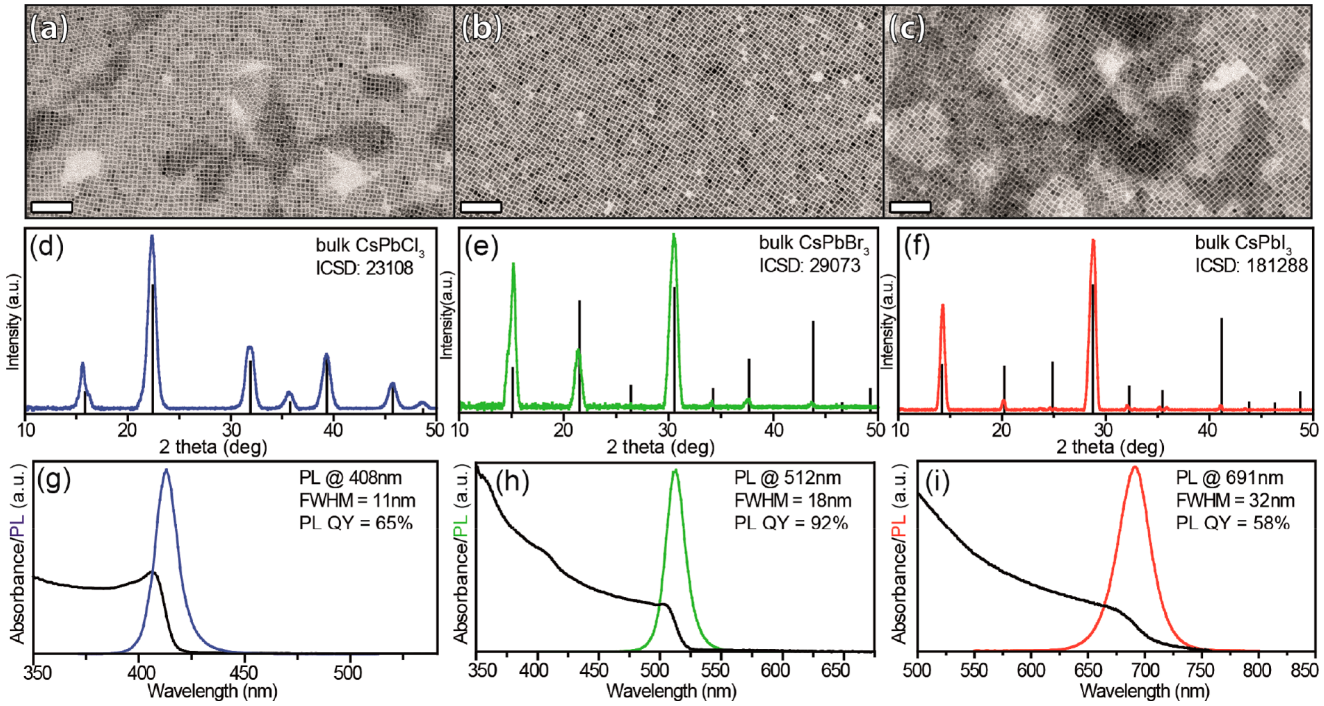

Figure 1. Bright-field TEM images of (a) $CsPbCl_3$, (b) $CsPbBr_3$, and (c) $CsPbI_3$ NCs. Scale bars are 100 nm in all images. XRD patterns of (d) $CsPbCl_3$, (e) $CsPbBr_3$, and (f) $CsPbI_3$ NCs along with the corresponding bulk cubic reference patterns. Absorption and PL spectra of (g) $CsPbCl_3$, (h) $CsPbBr_3$, and (i) $CsPbI_3$ NCs dispersed in toluene.

DOI: 10.1021/jacs.7b13477
J. Am. Chem. Soc. 2018, 140, 2656–2664

the Pb precursor led to NCs with a PLQY of just a few percentage points.

Time-correlated single-photon counting (TCSPC) measurements that were conducted on $APbX_3$ NCs revealed, as expected, that systems with higher band gaps had faster PL decay rates (see Figure S3a and Table S1 of the SI).[19] In particular, the calculated average lifetimes were 7.7 ns for $CsPbCl_3$ NCs, 12.5 ns for $CsPbBr_3$ NCs, and 21 ns for $CsPbI_3$ NCs. The average radiative and nonradiative decay rates that were estimated from the PLQYs and the average PL decay times are reported in Table S1 of the SI.

While, in general, lead halide-based perovskite NCs exhibit excellent optical properties, some of these materials are known for their poor structural stability. In particular, red-emitting $CsPbI_3$ NCs, the most interesting materials for photovoltaics applications, suffer from a delayed phase transformation from the metastable cubic (α) phase into the nonluminescent orthorhombic (δ) phase, also known as the "yellow phase".[58] For this reason, different approaches have been reported for the stabilization of the cubic phase, such as the use of alkyl phosphonic acids or phosphines in the synthesis of $CsPbI_3$ NCs,[47,48] washing procedures employing ethyl acetate,[28] replacing part of Cs^+ cations with bigger cations,[44] and replacing Pb^{2+} ions with Mn^{2+} cations.[49,50] In this regard, we observed that the cubic $CsPbI_3$ NCs that were synthesized with our procedure had a high phase stability, without any postsynthesis treatment. The XRD patterns of $CsPbI_3$ NC films exposed to air indicated that no phase transition occurred after 20 days (see Figure 2a).

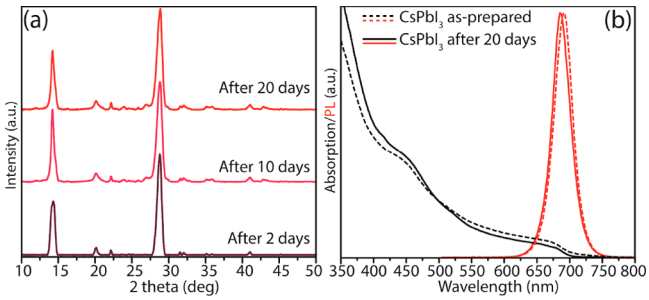

Figure 2. (a) XRD patterns and (b) UV–vis and PL curves of $CsPbI_3$ NCs exposed to air up to 20 days.

Furthermore, our optical characterizations of the NCs after air exposure confirmed the absence of the $CsPbI_3$ yellow phase, since no absorption features appeared at ~440 nm, which can be ascribed to the orthorhombic $CsPbI_3$ band-edge absoption,[59] and the NCs retained their PL emission (see Figure 2b).

In order to understand the reason behind the phase stability of $CsPbI_3$ NCs, and possibly also the PL properties of our $CsPbX_3$ NCs, we performed XPS characterization to study their surface and composition. The surface chemistry of lead halide-based perovskite NCs has been shown to play a fundamental role in determining not only their stability in air or under annealing, but also their optical performance.[17,28,60–64] The analysis of the Cs 3d, Pb 4f, and X peaks (Cl 2p, Br 3d, and I 3d) revealed that our $CsPbX_3$ NCs were substoichiometric in Cs, while the Pb:X ratio was always close to 3 (see Figure S4 of the SI). In more detail, the Cs:Pb:X ratios found in our NCs were: 0.9:1:3.1 in the case of chlorides, 0.8:1:2.8 in the case of bromides, and 0.8:1:2.7 in the case of iodides. We also roughly estimated the amount of oleylammonium ions bound to $CsPbX_3$ NCs by analyzing the N 1s peak (see Figure S4 of the SI). The chloride and bromide NCs had a ratio of Cs:N close to 1:0.5, and the iodide ones had a ratio of 1:1.2. These results suggest that the surface of our $CsPbX_3$ NCs is lead halide terminated, i.e., the surface Cs ions are replaced by oleylammonium ions. Lead halide perovskite NCs with this type of surface have been reported to have improved stability and enhanced optical properties.[29,63] Indeed, Woo et al. ascribed the improved stability of their $CsPbBr_3$ NCs (which were obtained with the hot-injection method, adding $ZnBr_2$ as an extra bromide source) to their lead bromide-rich surfaces.[29] In addition, Ravi et al. demonstrated that alkylmmonium ions have the ability to substitute Cs ions on the surface of $CsPbX_3$ NCs, which consequently improves their stability and optical properties.[63] We believe that our new synthetic procedure is favorable with regard to the formation of oleylammonium lead halide surfaces thanks to the halide-rich conditions that are used (see the Experimental Section). Moreover, the release of X^- ions from the acyl halides is accompanied by the concomitant release of H^+ ions, which can drive the protonation of the oleylamine in solution (see eqs 3–5).

As benzoyl halides can be easily mixed together, we also tested our procedure to synthesize mixed-halide NCs, namely, $CsPb(Cl/Br)_3$ and $CsPb(Br/I)_3$. These compounds as well as the starting $CsPbX_3$ NCs could be successfully synthesized with a narrow size distribution, phase purity, and good optical properties, simply by injecting mixtures of benzoyl halides in appropriate ratios (see Experimental Section and Figure S5 of the SI). Also, given the strong reactivity of benzoyl halides even at room temperature, we tested the $CsPbX_3$ NCs for postsynthesis transformations, namely, for anion-exchange reactions. Thus far, the most commonly used precursors for anion-exchange reactions have been metal halide salts (i.e., MX_2 where M = Pb, Zn, Mg, Cu, Ca and X = Cl, Br, I) and oleylammonium or tetrabutylammonium halides.[20–25] However, a disadvantage of these halide sources is that either they suffer from poor solubility in nonpolar solvents or their reactivity is limited at RT. On the contrary, benzoyl halides were observed to be efficient precursors for anion-exchange reactions: the addition of benzoyl chloride or benzoyl iodide to presynthesized $CsPbBr_3$ NCs led to a fast blue shift or red shift, respectively, of the peaks in both the PL and the absorption spectra of the NCs (see Figure 3, Experimental Section, and Figure S6a of the SI). In both cases, the XRD patterns of the resulting NCs confirmed the retention of the parent cubic perovskite structure, and there was a systematic shift of the peaks induced by the variation of the lattice parameters (see

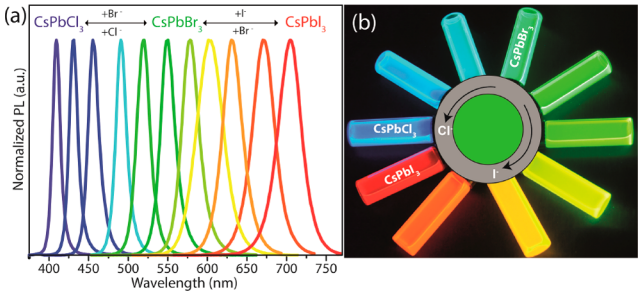

Figure 3. (a) Evolution of the PL spectra of $CsPbBr_3$ NCs by the addition of benzoyl chloride or benzoyl iodide. (b) Picture of the different $CsPbX_3$ NC solutions obtained by anion exchange under a UV lamp.

DOI: 10.1021/jacs.7b13477
J. Am. Chem. Soc. 2018, 140, 2656–2664

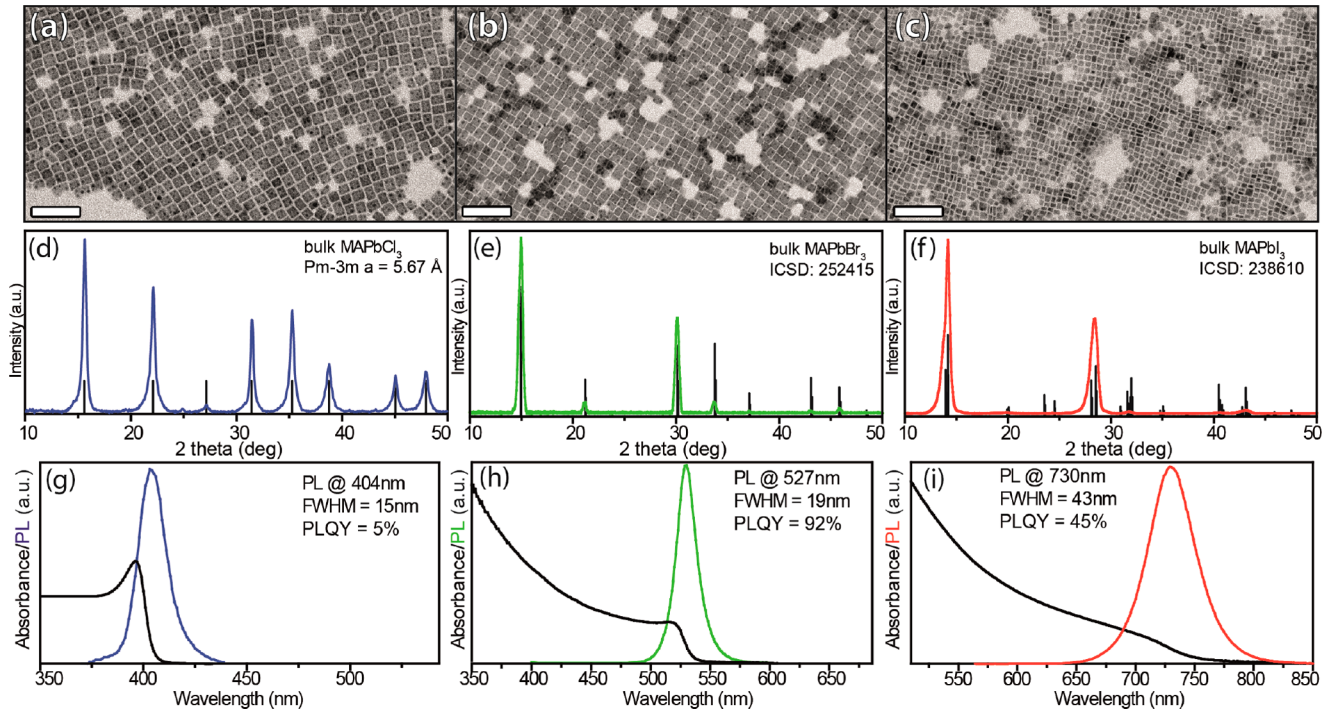

Figure 4. Bright-field TEM images of (a) $MAPbCl_3$, (b) $MAPbBr_3$, and (c) $MAPbI_3$ NCs. Scale bars are 100 nm in all images. XRD patterns of (d) $MAPbCl_3$, (e) $MAPbBr_3$, and (f) $MAPbI_3$ NCs along with their corresponding bulk cubic reference patterns. In the case of $MAPbCl_3$, the bulk reflections were calculated using the crystal structure that was reported by Maculan et al.[65] Absorption and PL spectra of (g) $MAPbCl_3$, (h) $MAPbBr_3$, and (i) $MAPbI_3$ NCs dispersed in toluene.

Figure S6b of the SI). Interestingly, the back-exchange reactions, $CsPbCl_3 \rightarrow CsPbBr_3$ and $CsPbI_3 \rightarrow CsPbBr_3$, also worked efficiently when benzoyl bromide was added to the $CsPbCl_3$ and $CsPBI_3$ NC solutions, respectively (see Figure S7 of the SI).

We then extended our protocol to the colloidal synthesis of hybrid organic–inorganic $APbX_3$ (A = MA, FA) perovskite NCs. We first tested our hot-injection approach by preparing $MAPbX_3$ NCs which, to date, have been mainly produced using the LARP technique since standard hot-injection techniques result in NCs with poor optical properties.[32] These hybrid organic–inorganic NCs could be synthesized using the protocol we devised for $CsPbX_3$ NCs, with only minor modifications (see Experimental Section). Bright-field TEM images of representative $MAPbX_3$ NCs are shown in Figure 4a–c. In all three cases, a nearly cubic morphology with a narrow size distribution was observed: the average length of the NCs was 20.1 ± 2.9 nm for $MAPbCl_3$, 15.5 ± 1.8 nm for $MAPbBr_3$, and 8.9 ± 2.4 nm for $MAPbI_3$ (see Figure 4a–c and Figure S8 of the SI). It is worth mentioning that PbO was used as the lead precursor for the synthesis of $MAPbX_3$ NCs instead of lead acetate as it enabled a better control over the size distribution and shape of the final NCs (see the Experimental Section and Figure S9 of the SI).

According to XRD analysis, the structure of the $MAPbBr_3$ NCs matched the cubic perovskite structure (ICSD code 252415) while that of $MAPbI_3$ NCs exhibited a tetragonal $CH_3NH_3PbI_3$ crystal phase (space group *I*4/*mcm*, ICSD code 238610). This is in agreement with a recent report by Zhang et al. on identical systems (see Figure 4e and 4f).[38] Given the absence of any reference pattern for $MAPbCl_3$ in the ICSD database, we compared the XRD pattern of our $MAPbCl_3$ NCs with those of bulk crystals that are reported in the literature, and we found a good match with that reported by Maculan et al., which is a cubic perovskite structure (space group *Pm*-3m) with a = 5.67 Å (see Figure 4d).[65,66]

The UV–vis absorption and PL spectra of $MAPbX_3$ NCs are shown in Figure 4g–i. Similar to what has been previously reported, all NC samples had a narrow PL emission with a fwhm of 15 nm for $MAPbCl_3$, 19 nm for $MAPbBr_3$, and 43 nm for $MAPbI_3$.[15,32,66] Remarkably, the $MAPbBr_3$ and $MAPbI_3$ NCs had a PLQY as high as 92% and 45%, respectively, while for $MAPbCl_3$ NCs the PLQY was around 5%. Similar to the case of $CsPbCl_3$ NCs, we did observe an enhancement of the PL emission of $MAPbCl_3$ NCs when increasing the amount of the Cl precursor to 1 mmol (see Figure S10a of the SI). Such improvement occurred along with the formation of a secondary undesired $PbCl_2$ phase (see Figure S10b of the SI). These findings suggest that, as in the case of $CsPbX_3$ systems, a lead halide-rich environment could enhance the PL emission of the resulting $MAPbCl_3$ NCs. Unfortunately, in this case such environment leads also to the formation of $PbCl_2$ which, thus, limits the effective amount of the Cl precursor that can be employed. Decay lifetimes, which were acquired by means of TCSPC measurements, were 5.4 ns for $MAPbCl_3$ NCs, 35 ns for $MAPbBr_3$ NCs, and 35.7 ns for $MAPbI_3$ NCs (see Figure S3b and Table S1 of the SI).

Although the synthesis of $MAPbX_3$ NCs has been optimized over the past few years, $FAPbX_3$ NCs with optimal optical properties as well as a narrow size distribution and phase purity have not yet been prepared by either hot-injection techniques or by the LARP approach.[18,40,44–46] Lately, these compounds have received considerable interest since they have several advantages over their methylammonium counterparts, such as a higher stability due to a more symmetric and tightly packed crystal structure.[67–69] We could also synthesize $FAPbX_3$ NCs

DOI: 10.1021/jacs.7b13477
J. Am. Chem. Soc. 2018, 140, 2656–2664

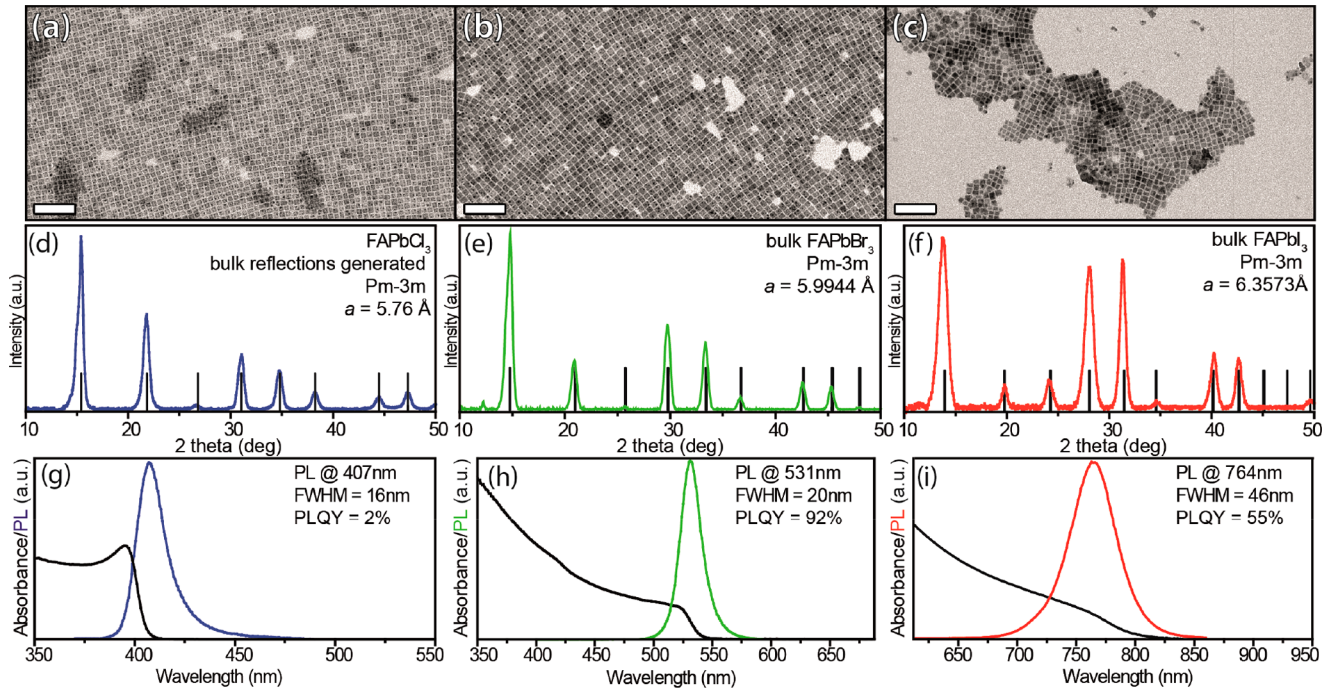

Figure 5. Bright-field TEM images of (a) $FAPbCl_3$, (b) $FAPbBr_3$, and (c) $FAPbI_3$ NCs. Scale bars are 100 nm in all images. XRD patterns of (d) $FAPbCl_3$, (e) $FAPbBr_3$, and (f) $FAPbI_3$ NCs along with the corresponding bulk cubic reference patterns. For $FAPbBr_3$ and $FAPbI_3$ NCs, the bulk reflections were calculated using the crystal structure reported by Zhumekenov et al.,[70] while the reflections of the $FAPbCl_3$ NCs were generated using a cubic perovskite structure (*Pm*-3m) with a = 5.76 Å. Absorption and PL spectra of (g) $FAPbCl_3$, (h) $FAPbBr_3$, and (i) $FAPbI_3$ NCs dispersed in toluene.

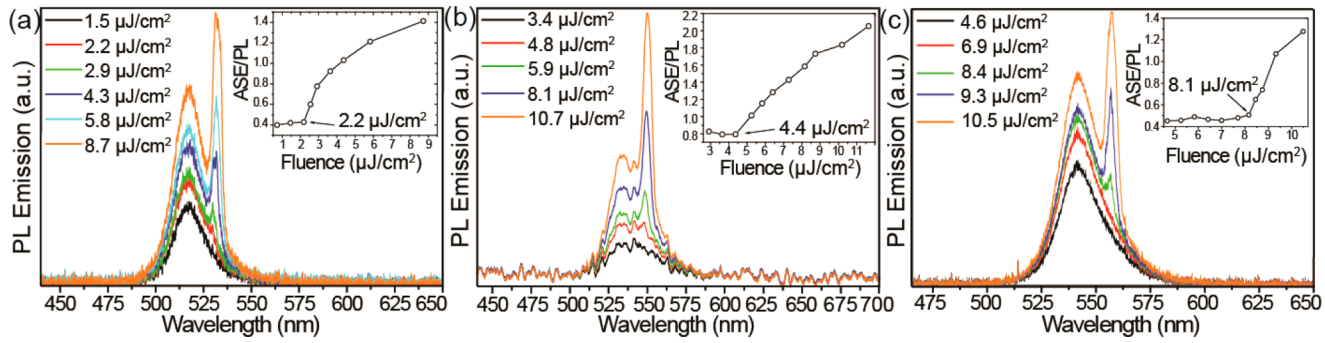

Figure 6. ASE dynamics for (a) $CsPbBr_3$, (b) $MAPbBr_3$, and (c) $FAPbBr_3$ together with the ASE threshold calculations (insets).

using our protocol (see Experimental Section). Typical TEM images of $FAPbCl_3$ and $FAPbBr_3$ NCs evidenced a narrow size distribution, which became slightly broader in the case of $FAPbI_3$ NCs (see Figure 5a–c and Figure S11 of the SI). The average size of the NCs was 11.2 ± 1.4 nm for $FAPbCl_3$, 12.4 ± 1.6 nm for $FAPbBr_3$, and 14.2 ± 2.8 nm for $FAPbI_3$. Regarding the structural analysis, given the absence of any $FAPbX_3$ reference patterns in the ICSD database, we had to compare the XRD patterns of our $FAPbX_3$ NCs with those of bulk crystals which have been recently published. In the case of $FAPbBr_3$ and $FAPbI_3$ NCs, a good match was found with the cubic structures reported by Zhumekenov et al.[70] (see Figure 5d–f). On the other hand, no cubic bulk structure has been reported so far for $FAPbCl_3$ compounds. This can be explained by its calculated tolerance factor (1.150), which in principle is too large to allow a 3D phase formation.[71] Conversely, the refinement of the XRD pattern of our $FAPbCl_3$ NCs led to a cubic structure (space group *Pm*-3m) with a = 5.67 Å. This represents the first report of a cubic $FAPbCl_3$ structure. UV–vis and PL spectra of the $FAPbX_3$ NCs are shown in Figure 5g–i. Furthermore, Br- and I-based compounds exhibited excellent optical properties and had a high PLQY (92% for $FAPbBr_3$ and 65% for $FAPbI_3$) and narrow PL emission (20 nm for $FAPbBr_3$ and 48 nm for $FAPbI_3$). The $FAPbCl_3$ NCs were characterized by having a narrow PL (fwhm = 16 nm) but a low PLQY (about 2%). Decay lifetimes, which were acquired by means of TCSPC measurements, were 14.8 ns for $FAPbCl_3$ NCs, 30.3 ns for $FAPbBr_3$ NCs, and 75.2 ns for $FAPbI_3$ NCs (see Figure S3c and Table S1 of the SI).

Finally, we investigated the amplified spontaneous emission (ASE) which occurred in the $APbBr_3$ NC films. These particular NCs had the highest PLQYs (more than 90% in all three of cases), much higher than those of their Cl and I counterparts ($APbCl_3$ and $APbI_3$). Figure 6a–c reports the emission spectra showing ASE of the three $APbBr_3$ NC samples together with the ASE thresholds. All three systems manifested very low ASE thresholds, ranging from 2.2 to 8.1 $\mu J/cm^2$, which are either comparable to or lower than the lowest values that

DOI: 10.1021/jacs.7b13477
J. Am. Chem. Soc. 2018, 140, 2656–2664

have been reported in the literature (see Table S2).[72] Moreover, all three of the systems had very narrow ASE fwhm due to the very narrow gain in bandwidth (See Figure S12 of the SI).[73]

CONCLUSIONS

We have demonstrated a new colloidal route for the preparation of both all-inorganic and hybrid organic−inorganic $APbX_3$ NCs (A = Cs, MA, FA and X = Cl, Br, I). Our approach is based on the injection of benzoyl halides (as halide precursors) into a solution of desired cations and proper ligands (oleylamine and oleic acid) at a desired temperature. After the injection, a fast release of halide ions occurs, which is followed by the nucleation and growth of metal halide NCs. In all cases, the resulting $APbX_3$ NCs show a high phase stability, a very good size distribution, and excellent optical properties. They exhibit a narrow PL emission and high PLQYs, which are around 90% in the case of $APbBr_3$ systems, 55% in the case of $APbI_3$ materials, and a record value of 65% in the case if $CsPbCl_3$ NCs. The optical quality of our materials was also reflected by the low values of their ASE thresholds. The origin of such improvements with regard to the stability and optical properties of $CsPbX_3$ NCs was tentatively ascribed to the formation of lead halide-terminated surfaces in which Cs ions are partially replaced by oleylammonium ions. Indeed, the formation of such surfaces is promoted by our synthetic conditions. To conclude, we believe that the versatility of our synthetic approach will allow for the future development of all-inorganic and organic−inorganic lead-free metal halide NC systems.

ASSOCIATED CONTENT

Supporting Information

The Supporting Information is available free of charge on the ACS Publications website at DOI: 10.1021/jacs.7b13477.

NMR characterization of benzoyl iodide, size distribution of all of the $APbX_3$ NCs, time-resolved spectroscopic characterization, control experiments on $MAPbCl_3$ NCs, XPS analysis, $CsPb(Br/I)_3$, and $CsPb(Cl/Br)_3$ NCs, anion-exchange results, $MAPbBr_3$ NCs synthesized with lead acetate trihydrate, overview of reported ASE thresholds (PDF)

AUTHOR INFORMATION

Corresponding Authors

*luca.detrizio@iit.it

*liberato.manna@iit.it

ORCID

Muhammad Imran: 0000-0001-7091-6514

Vincenzo Caligiuri: 0000-0003-1035-4702

Mirko Prato: 0000-0002-2188-8059

Roman Krahne: 0000-0003-0066-7019

Luca De Trizio: 0000-0002-1514-6358

Liberato Manna: 0000-0003-4386-7985

Notes

The authors declare no competing financial interest.

ACKNOWLEDGMENTS

We acknowledge funding from the European Union under grant agreement no. 614897 (ERC Grant TRANS-NANO).

REFERENCES

(1) Huang, H.; Bodnarchuk, M. I.; Kershaw, S. V.; Kovalenko, M. V.; Rogach, A. L. *ACS Energy Lett.* **2017**, *2*, 2071−2083.

(2) Li, X.; Wu, Y.; Zhang, S.; Cai, B.; Gu, Y.; Song, J.; Zeng, H. *Adv. Funct. Mater.* **2016**, *26*, 2435−2445.

(3) He, X.; Qiu, Y.; Yang, S. *Adv. Mater.* **2017**, *29*, 1700775.

(4) Ono, L. K.; Juarez-Perez, E. J.; Qi, Y. *ACS Appl. Mater. Interfaces* **2017**, *9*, 30197−30246.

(5) Giustino, F.; Snaith, H. J. *ACS Energy Lett.* **2016**, *1*, 1233−1240.

(6) Zhao, X.-G.; Yang, J.-H.; Fu, Y.; Yang, D.; Xu, Q.; Yu, L.; Wei, S.-H.; Zhang, L. *J. Am. Chem. Soc.* **2017**, *139*, 2630−2638.

(7) Amgar, D.; Aharon, S.; Etgar, L. *Adv. Funct. Mater.* **2016**, *26*, 8576−8593.

(8) Manser, J. S.; Christians, J. A.; Kamat, P. V. *Chem. Rev.* **2016**, *116*, 12956−13008.

(9) Huang, H.; Polavarapu, L.; Sichert, J. A.; Susha, A. S.; Urban, A. S.; Rogach, A. L. *NPG Asia Mater.* **2016**, *8*, e328.

(10) Bai, S.; Yuan, Z.; Gao, F. *J. Mater. Chem. C* **2016**, *4*, 3898−3904.

(11) Fu, P.; Shan, Q.; Shang, Y.; Song, J.; Zeng, H.; Ning, Z.; Gong, J. *Sci. Bull.* **2017**, *62*, 369−380.

(12) Kovalenko, M. V.; Protesescu, L.; Bodnarchuk, M. I. *Science* **2017**, *358*, 745−750.

(13) Adjokatse, S.; Fang, H.-H.; Loi, M. A. *Mater. Today* **2017**, *20*, 413−424.

(14) Hu, F.; Zhang, H.; Sun, C.; Yin, C.; Lv, B.; Zhang, C.; Yu, W. W.; Wang, X.; Zhang, Y.; Xiao, M. *ACS Nano* **2015**, *9*, 12410−12416.

(15) Gonzalez-Carrero, S.; Francés-Soriano, L.; González-Béjar, M.; Agouram, S.; Galian, R. E.; Pérez-Prieto, J. *Small* **2016**, *12*, 5245−5250.

(16) Kim, Y.; Yassitepe, E.; Voznyy, O.; Comin, R.; Walters, G.; Gong, X.; Kanjanaboos, P.; Nogueira, A. F.; Sargent, E. H. *ACS Appl. Mater. Interfaces* **2015**, *7*, 25007−25013.

(17) Koscher, B. A.; Swabeck, J. K.; Bronstein, N. D.; Alivisatos, A. P. *J. Am. Chem. Soc.* **2017**, *139*, 6566−6569.

(18) Levchuk, I.; Osvet, A.; Tang, X.; Brandl, M.; Perea, J. D.; Hoegl, F.; Matt, G. J.; Hock, R.; Batentschuk, M.; Brabec, C. J. *Nano Lett.* **2017**, *17*, 2765−2770.

(19) Protesescu, L.; Yakunin, S.; Bodnarchuk, M. I.; Krieg, F.; Caputo, R.; Hendon, C. H.; Yang, R. X.; Walsh, A.; Kovalenko, M. V. *Nano Lett.* **2015**, *15*, 3692−3696.

(20) Zhang, T.; Li, G.; Chang, Y.; Wang, X.; Zhang, B.; Mou, H.; Jiang, Y. *CrystEngComm* **2017**, *19*, 1165−1171.

(21) Akkerman, Q. A.; D'Innocenzo, V.; Accornero, S.; Scarpellini, A.; Petrozza, A.; Prato, M.; Manna, L. *J. Am. Chem. Soc.* **2015**, *137*, 10276−10281.

(22) Guhrenz, C.; Benad, A.; Ziegler, C.; Haubold, D.; Gaponik, N.; Eychmüller, A. *Chem. Mater.* **2016**, *28*, 9033−9040.

(23) Nedelcu, G.; Protesescu, L.; Yakunin, S.; Bodnarchuk, M. I.; Grotevent, M. J.; Kovalenko, M. V. *Nano Lett.* **2015**, *15*, 5635−5640.

(24) De Trizio, L.; Manna, L. *Chem. Rev.* **2016**, *116*, 10852−10887.

(25) Parobek, D.; Dong, Y.; Qiao, T.; Rossi, D.; Son, D. H. *J. Am. Chem. Soc.* **2017**, *139*, 4358−4361.

(26) Dou, L. *J. Mater. Chem. C* **2017**, *5*, 11165−11173.

(27) Ning, C.-Z.; Dou, L.; Yang, P. *Nat. Rev. Mater.* **2017**, *2*, 17070.

(28) Swarnkar, A.; Marshall, A. R.; Sanehira, E. M.; Chernomordik, B. D.; Moore, D. T.; Christians, J. A.; Chakrabarti, T.; Luther, J. M. *Science* **2016**, *354*, 92−95.

(29) Woo, J. Y.; Kim, Y.; Bae, J.; Kim, T. G.; Kim, J. W.; Lee, D. C.; Jeong, S. *Chem. Mater.* **2017**, *29*, 7088−7092.

(30) Koolyk, M.; Amgar, D.; Aharon, S.; Etgar, L. *Nanoscale* **2016**, *8*, 6403−6409.

(31) Li, G.; Wang, H.; Zhang, T.; Mi, L.; Zhang, Y.; Zhang, Z.; Zhang, W.; Jiang, Y. *Adv. Funct. Mater.* **2016**, *26*, 8478−8486.

(32) Vybornyi, O.; Yakunin, S.; Kovalenko, M. V. *Nanoscale* **2016**, *8*, 6278−6283.

(33) Jellicoe, T. C.; Richter, J. M.; Glass, H. F. J.; Tabachnyk, M.; Brady, R.; Dutton, S. E.; Rao, A.; Friend, R. H.; Credgington, D.; Greenham, N. C.; Böhm, M. L. *J. Am. Chem. Soc.* **2016**, *138*, 2941−2944.

DOI: 10.1021/jacs.7b13477
J. Am. Chem. Soc. 2018, 140, 2656−2664

(34) Sun, S.; Yuan, D.; Xu, Y.; Wang, A.; Deng, Z. *ACS Nano* **2016**, *10*, 3648−3657.
(35) Kumar, S.; Jagielski, J.; Yakunin, S.; Rice, P.; Chiu, Y.-C.; Wang, M.; Nedelcu, G.; Kim, Y.; Lin, S.; Santos, E. J. G.; Kovalenko, M. V.; Shih, C.-J. *ACS Nano* **2016**, *10*, 9720−9729.
(36) Schmidt, L. C.; Pertegás, A.; González-Carrero, S.; Malinkiewicz, O.; Agouram, S.; Mínguez Espallargas, G.; Bolink, H. J.; Galian, R. E.; Pérez-Prieto, J. *J. Am. Chem. Soc.* **2014**, *136*, 850−853.
(37) Zhang, F.; Zhong, H.; Chen, C.; Wu, X.-g.; Hu, X.; Huang, H.; Han, J.; Zou, B.; Dong, Y. *ACS Nano* **2015**, *9*, 4533−4542.
(38) Zhang, F.; Huang, S.; Wang, P.; Chen, X.; Zhao, S.; Dong, Y.; Zhong, H. *Chem. Mater.* **2017**, *29*, 3793−3799.
(39) Levchuk, I.; Herre, P.; Brandl, M.; Osvet, A.; Hock, R.; Peukert, W.; Schweizer, P.; Spiecker, E.; Batentschuk, M.; Brabec, C. J. *Chem. Commun.* **2017**, *53*, 244−247.
(40) Minh, D. N.; Kim, J.; Hyon, J.; Sim, J. H.; Sowlih, H. H.; Seo, C.; Nam, J.; Eom, S.; Suk, S.; Lee, S.; Kim, E.; Kang, Y. *Chem. Mater.* **2017**, *29*, 5713−5719.
(41) Kang, J.; Wang, L.-W. *J. Phys. Chem. Lett.* **2017**, *8*, 489−493.
(42) Wei, S.; Yang, Y.; Kang, X.; Wang, L.; Huang, L.; Pan, D. *Chem. Commun.* **2016**, *52*, 7265−7268.
(43) Yassitepe, E.; Yang, Z.; Voznyy, O.; Kim, Y.; Walters, G.; Castañeda, J. A.; Kanjanaboos, P.; Yuan, M.; Gong, X.; Fan, F.; Pan, J.; Hoogland, S.; Comin, R.; Bakr, O. M.; Padilha, L. A.; Nogueira, A. F.; Sargent, E. H. *Adv. Funct. Mater.* **2016**, *26*, 8757−8763.
(44) Protesescu, L.; Yakunin, S.; Kumar, S.; Bär, J.; Bertolotti, F.; Masciocchi, N.; Guagliardi, A.; Grotevent, M.; Shorubalko, I.; Bodnarchuk, M. I.; Shih, C.-J.; Kovalenko, M. V. *ACS Nano* **2017**, *11*, 3119−3134.
(45) Protesescu, L.; Yakunin, S.; Bodnarchuk, M. I.; Bertolotti, F.; Masciocchi, N.; Guagliardi, A.; Kovalenko, M. V. *J. Am. Chem. Soc.* **2016**, *138*, 14202−14205.
(46) Li, Q.; Li, H.; Shen, H.; Wang, F.; Zhao, F.; Li, F.; Zhang, X.; Li, D.; Jin, X.; Sun, W. *ACS Photonics* **2017**, *4*, 2504−2512.
(47) Wang, C.; Chesman, A. S. R.; Jasieniak, J. J. *Chem. Commun.* **2017**, *53*, 232−235.
(48) Liu, F.; Zhang, Y.; Ding, C.; Kobayashi, S.; Izuishi, T.; Nakazawa, N.; Toyoda, T.; Ohta, T.; Hayase, S.; Minemoto, T.; Yoshino, K.; Dai, S.; Shen, Q. *ACS Nano* **2017**, *11*, 10373−10383.
(49) Zou, S.; Liu, Y.; Li, J.; Liu, C.; Feng, R.; Jiang, F.; Li, Y.; Song, J.; Zeng, H.; Hong, M.; Chen, X. *J. Am. Chem. Soc.* **2017**, *139*, 11443−11450.
(50) Akkerman, Q. A.; Meggiolaro, D.; Dang, Z.; De Angelis, F.; Manna, L. *ACS Energy Lett.* **2017**, *2*, 2183−2186.
(51) Theobald, D. W.; Smith, J. C. *Chem. Ind.* **1958**, *32*, 1007−1008.
(52) Ito, D.; Yokoyama, S.; Zaikova, T.; Masuko, K.; Hutchison, J. E. *ACS Nano* **2014**, *8*, 64−75.
(53) Patai, S. John Wiley & Sons Ltd: UK, 1972.
(54) Hoffmann, H. M. R.; Haase, K. *Synthesis* **1981**, *1981*, 715−719.
(55) Harris, D. K.; Bawendi, M. G. *J. Am. Chem. Soc.* **2012**, *134*, 20211−20213.
(56) Voronkov, M. G.; Tsyrendorzhieva, I. P.; Lis, A. V.; Grinberg, E. E.; Shatokhina, V. A.; Rakhlin, V. I. *Russ. J. Org. Chem.* **2013**, *49*, 147−150.
(57) Tong, Y.; Bladt, E.; Aygüler, M. F.; Manzi, A.; Milowska, K. Z.; Hintermayr, V. A.; Docampo, P.; Bals, S.; Urban, A. S.; Polavarapu, L.; Feldmann, J. *Angew. Chem., Int. Ed.* **2016**, *55*, 13887−13892.
(58) Trots, D. M.; Myagkota, S. V. *J. Phys. Chem. Solids* **2008**, *69*, 2520−2526.
(59) Kim, Y. G.; Kim, T.-Y.; Oh, J. H.; Choi, K. S.; Kim, Y.-J.; Kim, S. Y. *Phys. Chem. Chem. Phys.* **2017**, *19*, 6257−6263.
(60) Pan, A.; He, B.; Fan, X.; Liu, Z.; Urban, J. J.; Alivisatos, A. P.; He, L.; Liu, Y. *ACS Nano* **2016**, *10*, 7943−7954.
(61) Giansante, C.; Infante, I. *J. Phys. Chem. Lett.* **2017**, *8*, 5209−5215.
(62) Pan, J.; Sarmah, S. P.; Murali, B.; Dursun, I.; Peng, W.; Parida, M. R.; Liu, J.; Sinatra, L.; Alyami, N.; Zhao, C.; Alarousu, E.; Ng, T. K.; Ooi, B. S.; Bakr, O. M.; Mohammed, O. F. *J. Phys. Chem. Lett.* **2015**, *6*, 5027−5033.
(63) Ravi, V. K.; Santra, P. K.; Joshi, N.; Chugh, J.; Singh, S. K.; Rensmo, H.; Ghosh, P.; Nag, A. *J. Phys. Chem. Lett.* **2017**, *8*, 4988−4994.
(64) De Roo, J.; Ibáñez, M.; Geiregat, P.; Nedelcu, G.; Walravens, W.; Maes, J.; Martins, J. C.; Van Driessche, I.; Kovalenko, M. V.; Hens, Z. *ACS Nano* **2016**, *10*, 2071−2081.
(65) Maculan, G.; Sheikh, A. D.; Abdelhady, A. L.; Saidaminov, M. I.; Haque, M. A.; Murali, B.; Alarousu, E.; Mohammed, O. F.; Wu, T.; Bakr, O. M. *J. Phys. Chem. Lett.* **2015**, *6*, 3781−3786.
(66) Shamsi, J.; Abdelhady, A. L.; Accornero, S.; Arciniegas, M.; Goldoni, L.; Kandada, A. R. S.; Petrozza, A.; Manna, L. *ACS Energy Lett.* **2016**, *1*, 1042−1048.
(67) Pellet, N.; Gao, P.; Gregori, G.; Yang, T.-Y.; Nazeeruddin, M. K.; Maier, J.; Grätzel, M. *Angew. Chem., Int. Ed.* **2014**, *53*, 3151−3157.
(68) Eperon, G. E.; Stranks, S. D.; Menelaou, C.; Johnston, M. B.; Herz, L. M.; Snaith, H. J. *Energy Environ. Sci.* **2014**, *7*, 982−988.
(69) Amat, A.; Mosconi, E.; Ronca, E.; Quarti, C.; Umari, P.; Nazeeruddin, M. K.; Grätzel, M.; De Angelis, F. *Nano Lett.* **2014**, *14*, 3608−3616.
(70) Zhumekenov, A. A.; Saidaminov, M. I.; Haque, M. A.; Alarousu, E.; Sarmah, S. P.; Murali, B.; Dursun, I.; Miao, X.-H.; Abdelhady, A. L.; Wu, T.; Mohammed, O. F.; Bakr, O. M. *ACS Energy Lett.* **2016**, *1*, 32−37.
(71) Becker, M.; Kluner, T.; Wark, M. *Dalton Trans.* **2017**, *46*, 3500−3509.
(72) Veldhuis, S. A.; Tay, Y. K. E.; Bruno, A.; Dintakurti, S. S. H.; Bhaumik, S.; Muduli, S. K.; Li, M.; Mathews, N.; Sum, T. C.; Mhaisalkar, S. G. *Nano Lett.* **2017**, *17*, 7424−7432.
(73) Yakunin, S.; Protesescu, L.; Krieg, F.; Bodnarchuk, M. I.; Nedelcu, G.; Humer, M.; De Luca, G.; Fiebig, M.; Heiss, W.; Kovalenko, M. V. *Nat. Commun.* **2015**, *6*, 8056.

DOI: 10.1021/jacs.7b13477
J. Am. Chem. Soc. 2018, 140, 2656−2664